

## New Worlds Ahead: The Discovery of Exoplanets

Arnaud CASSAN  
Université Pierre et Marie Curie  
Institut d'Astrophysique de Paris  
98bis boulevard Arago  
75014 Paris, France

**Abstract.** Exoplanets are planets orbiting stars other than the Sun. In 1995, the discovery of the first exoplanet orbiting a solar-type star paved the way to an exoplanet detection rush, which revealed an astonishing diversity of possible worlds. These detections led us to completely renew planet formation and evolution theories. Several detection techniques have revealed a wealth of surprising properties characterizing exoplanets that are not found in our own planetary system. After two decades of exoplanet search, these new worlds are found to be ubiquitous throughout the Milky Way. A positive sign that life has developed elsewhere than on Earth?

### 1 The Solar system paradigm: the end of certainties

Looking at the Solar system, striking facts appear clearly: all seven planets orbit in the same plane (the ecliptic), all have almost circular orbits, the Sun rotation is perpendicular to this plane, and the direction of the Sun rotation is the same as the planets revolution around the Sun.

These observations gave birth to the Solar nebula theory, which was proposed by Kant and Laplace more than two hundred years ago, but, although correct, it has been for decades the subject of many debates. In this theory, the Solar system was formed by the collapse of an approximately spheric giant interstellar cloud of gas and dust, which eventually flattened in the plane perpendicular to its initial rotation axis. The denser material in the center collapsed further under self-gravity, increased in density and formed the Sun. Outside, the material had collapsed into a disk-shaped nebula, a gaseous flattened disk in differential rotation, where planets were supposed to form. An argument for that was that without planets orbiting the central star, the star's angular momentum would be so high that it would be disrupted by its own rotation speed, so in a sense planets were required.

Planets were therefore considered by a number of authors (notably Giordano Bruno) as by-products of a the global process of star formation, and the plurality of worlds was inferred as a natural consequence of the plurality of stars. First evidences that planet formation takes place in a proto-planetary disk composed of gas and dust were supported by observations of flux excess in the infrared and ultraviolet wavelengths, attributed to nebulae surrounding stars.

Another important fact about the Solar system lies in the arrangement of the planets around the Sun: the small, rocky planets Mercury, Venus, Earth and Mars are located at small orbital distances (less than 1.5 the Sun-Earth distance, or AU),

gas giant planets like Jupiter ( $318 M_{\oplus}$ ) and Saturn ( $95 M_{\oplus}$ ) are located further away (5 and 10 AU), and finally the icy giants Uranus and Neptune, located even further (20 and 30 AU), are much less massive ( $14 M_{\oplus}$  and  $17 M_{\oplus}$ ). Pluto does not fit well in this picture, but in fact it is not considered anymore as a planet – it is more a heavy version of an asteroid, today classified as a dwarf planet, with a very different history.

A relatively simple planet formation theory can explain most of these characteristics, and was widely accepted amongst the scientific community until the first exoplanet was detected in 1995. To grow large gaseous planets, it is necessary that there is enough material available around. This requires that the orbit is large, because the amount of material inside the feeding ring of the planet is higher, and because the temperature is low enough to allow the condensation of ices, which increases the solid fraction of the material and ease the nucleation process. Jupiter and Saturn are in fact located beyond the snow line, which delimits the orbit at which most ices condense (water, methane, ...). Orbits which are too far away suffer from the fact planets take more time to accomplish a given number of orbits, and thus accrete less gas before it falls in the star or is dispersed away by the stellar wind. Saturn is less massive than Jupiter, Uranus and Neptune are even lighter and contain a high fraction of ices. Small planets are found in relatively close orbits, because they have little material to accrete. All pieces of the puzzle made sense: Solar systems planets were formed *in situ*, at the orbital position they are seen today.

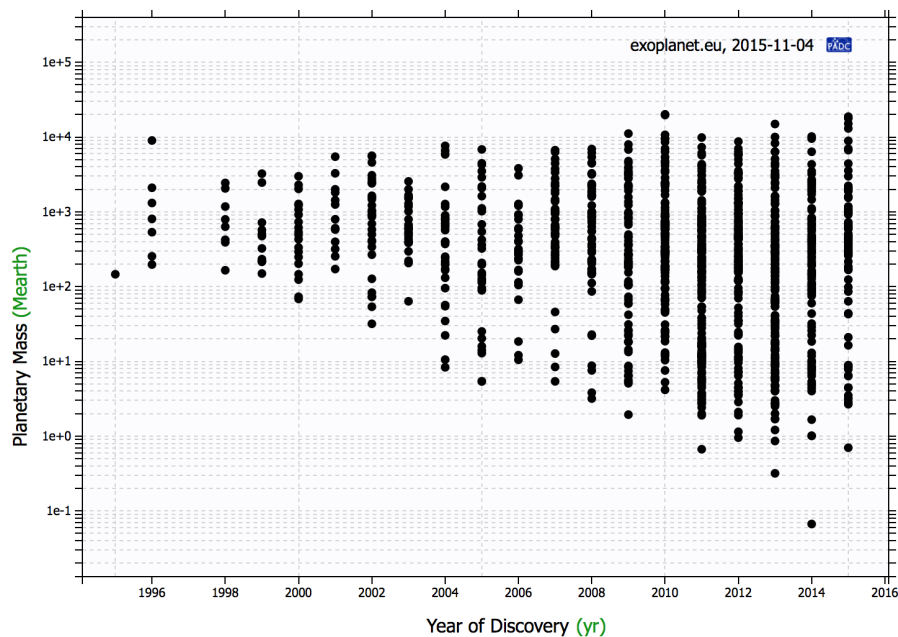


Figure 1: Exoplanet detections as a function of time since the discovery of 51 Peg b in 1995. The vertical axis displays the planetary mass in Earth masses, and shows the great improvements towards low masses with years, today down to that of the Earth (figure created with `exoplanet.eu`).

The paradigm that emerged from the observation of the Solar system was believed to also apply to other exo-planetary systems. The ideas behind it made the basis of the design of the first campaigns of exoplanet searches: find a Jupiter-like

planet located a few AU from another star than the Sun. But the first exoplanet detected around a star similar to the Sun, 51 Peg b, was definitely not of that kind: although not different in nature from Jupiter (it was a gas giant), its orbit of only 4 days period against 12 years for Jupiter caused a great surprise: it was a *hot* Jupiter! The formation of this exoplanet *in situ* was clearly ruled out: too hot, not enough material.

Hence the only possibility was that the planet had formed at a larger orbital distance, and eventually migrated inward to get close to the star via an adequate mechanism. It finally stopped at its current location and narrowly avoided to be swallowed by the star. The discovery of this unexpected hot Jupiter immediately generated a feverish research activity: those who did not believe in the planetary interpretation worked out new stellar pulsation theories; others investigated theoretical and numerical scenarios for planetary migration in the proto-planetary disk, and actually re-discovered calculations made at the turn of the 1970s.

Today, not only the classical Solar system formation scenario described above cannot accommodate the discovery of exoplanets, but the history of the Solar system itself has undergone significant changes. One of such popular theory is the Grand Tack model (or Nice model) which proposes that Jupiter migrated inward to 1.5 AU from an initial 5 AU formation orbit, and then migrated back outward due to disk torques before and after Saturn's formation. This scenario can account for another important aspect: the delivery of water on Earth (and other terrestrial planets) in the form of water-rich planetesimals (today still present in the asteroid belt as water-rich asteroids) scattered inward during the gas giants' outward migration.

The first exoplanet detections have triggered an unprecedented rush to detect exoplanets (Fig. 1), which provide essential (indispensable) information to understand their great diversity or their physical properties. We still make amazing discoveries 20 years after the first detection.

## 2 Searching for exoplanets

The detection of extrasolar planets has always been a great observational challenge, because the angular separation between the planet and the host star is extremely small and because the brightness contrast is extremely high. At the beginning of the 1990s, the only example of a planetary system was our Solar system. The first exoplanets have been discovered by indirect methods. In 1992, the timing of the millisecond pulsar PSR1257+12 led to the discovery of planetary-mass objects around a neutron star. A few years later, the first exoplanet orbiting a Sun-like star, 51 Peg b, was discovered by high-accuracy radial velocity measurements of the star's periodic motion. These two landmark discoveries have initiated a novel, very active field in astrophysics: the search and characterization of extrasolar planets. At the end of 2013, the exoplanet catalogue passed the symbolic 1000th entry. The number of detections has reached almost 2000 detections today.

The search for extra-solar planets have unveiled a striking fact: the great diversity of their physical properties. To introduce the main detection methods that are described in the coming paragraphs, the discoveries as of September 2015 are shown in the mass vs. semi-major axis diagram shown in Fig. 2.

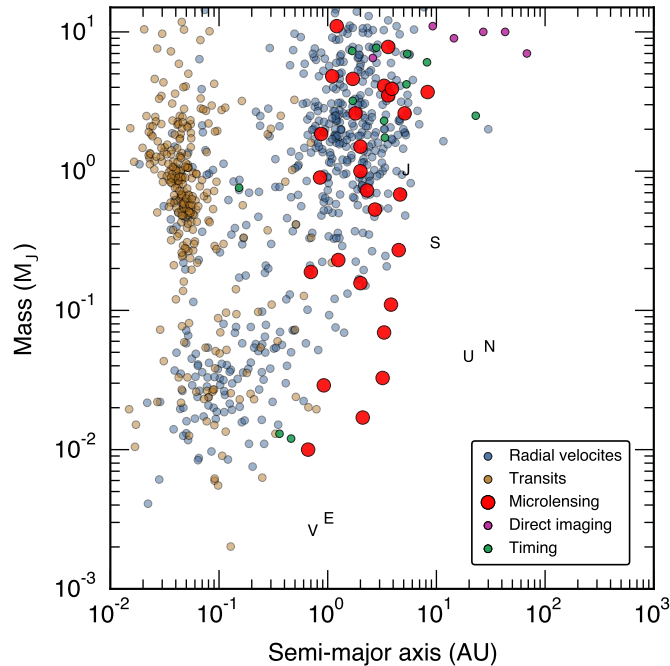


Figure 2: Exoplanet detections as of September 2015 with the main techniques described in the text, in a mass vs. semi-major axis diagram (Fig. courtesy C. Ranc).

## 2.1 Pulsar timing

In 1967, J. Bell and A. Hewish discovered in the sky the first member of a new kind of radio pulsating point-like sources that were called “pulsating stars”, or pulsars. It soon after became clear, however, that these objects had little to do with real stars, but that they were rapidly rotating and highly magnetized neutrons stars, whose existence was then subject to speculation. A neutron star is the remnant of a very massive star after it exploded as a supernova. While the original envelope of the star is blown away, its core collapses very fast and the pressure becomes so high that protons and electrons cannot resist it and merge to form neutrons. The equivalent of the mass of the Sun is contained inside a sphere of only 20 km in diameter. A pulsar is a magnetized neutron star which emits powerful radio waves in two cone-shaped beams which are inclined with respect to the spin axis. Every time a cone points toward the Earth, a pulse is received. Their typical periods range from milliseconds to seconds.

It was soon realized that the pulsation period of the pulsars was intrinsically extremely stable (millisecond pulsars did actually serve as time references). This property was first used in 1974 by J. Taylor and R. Hulse who showed indirectly that PSR1913+16 (a binary neutron star including a pulsar) emitted gravitational waves as predicted by the theory of General Relativity: the gravitational loss of energy shrinks the orbits of the companions, which in turn shortens the period of the pulses. Pulsars surveys were subsequently carried out with increasingly large radio telescopes.

In early 1990, the routine operations at the Arecibo radio telescope were shut down for repairs of the damages caused by material fatigue that had developed

over time. The astronomer A. Wolszczan took this opportunity to propose a large survey to discover new pulsars and probe the distribution of old neutron stars over the sky. The limited access to the telescope during the reparation phase made it practically unavailable to outside observers, and a large amount of time was granted to conduct his project. After a few months of monitoring, two new pulsars were found: one was part of a binary neutron star, while the second one, PSR B1257+12, was a millisecond pulsar with a spin period of 6.2 ms. The timing model of the latter did not fit well that of an isolated rotating neutron star, though. After several unsuccessful months spent in trying to refine the model, mid-1991, the pulsar was monitored during three weeks on a daily basis in order to track down the details of the discrepancy between the timing prediction and the actual observations. The pulse arrival times were found to trace a smooth curve (upper panel of Fig. 3), which was finally interpreted as a sign of a periodic phenomenon affecting the pulsar.

If the pulsar was perturbed by an orbiting companion such as a white dwarf (also a stellar remnant, but for a least massive progenitor star) as it was *a priori* the most likely interpretation, its reflex motion should translate into Doppler shifts of the apparent pulsar period. For a single Keplerian orbit, the varying delay  $\Delta t_R$  between pulses is given by

$$\Delta t_R = x(\cos E - e) \sin \omega + x \sin E \sqrt{1 - e^2} \cos \omega, \quad (1)$$

where  $x = (a \sin i)/c$ ,  $c$  is the speed of light,  $a$  is the semi-major axis,  $i$  is the orbital inclination,  $e$  is the eccentricity,  $E$  is the eccentric anomaly related to the mean anomaly  $M = (2\pi/P)(t - t_p)$  through  $M = E - e \sin E$ ,  $P$  is the orbital period,  $t_p$  is the time of the periastron passage and  $\omega$  is the periastron longitude. The amplitude of the variation, however, implied a companion of terrestrial mass several order of magnitudes smaller than the mass of a white dwarf (pulsar timing is so sensitive that even asteroid-mass bodies are detectable, equivalent to  $1 \text{ cm.s}^{-1}$  in Doppler precision).

The detailed analysis finally revealed the presence of two terrestrial planets (about three and four times the mass of the Earth) around pulsar PSR B1257+12 at the time of the publication in 1992 [29]. This configuration provided a quasi-perfect fit the varying delay between the pulses, as can be seen in the lower panel of Fig. 3, which exhibits almost no residuals for the initial 18 months of data. Later in 1994, a third, Moon-mass planet was found to orbit the pulsar too, at a closer orbit.

Hence, and very unexpectedly, the first planetary-mass objects have been found around a stellar remnant (sometimes called dead star), and not around a normal star as it was commonly expected. Nevertheless, the possible existence of planets around pulsars had been investigated shortly after the first pulsar discoveries [18], and two pulsar-planets were announced and later retracted before the discovery of PSR B1257+12. The story says that the announcement of the detection of planets around pulsar PSR1829-10 [3] and around PSR B1257+12 were programmed at the same conference, but the authors finally retracted their claim in public just before the announcement of the PSR B1257+12 planets. A second pulsar-planet system was finally discovered two years later [2].

The discovery of planets around pulsars provide a strong support that exoplanets exist around stars at all stages of their evolution, even in their final ones. Whether these planets have been formed from the fallback accretion of matter left

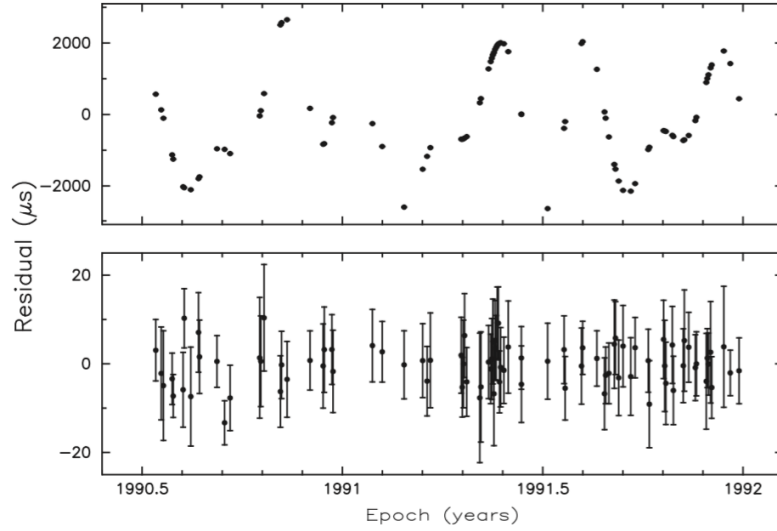


Figure 3: The upper panel shows the residuals of the pulse arrival times for the best pulsar timing model without companion (large residuals), while the lower panel is the same as above but including two companion terrestrial planets (figure from [29]).

in a post-supernova debris disk, as suggested by the quasi-planar architecture of the three planets around PSR B1257+12, or whether (although it is less likely) they are objects that have survived the explosion is not clear yet. The detection so far of only two planetary systems around millisecond pulsars means that building up planets around pulsars is not a common process, but it also supports the idea that the formation of terrestrial planets is an efficient process even in unfavorable environments.

## 2.2 Doppler spectroscopy

The first exoplanet orbiting a normal star (*i.e.* a star burning mainly hydrogen as its source of heat, like the Sun) was discovered in 1995 by Doppler spectroscopy of its host star. It has remained the most productive detection technique for about 20 years, before space missions dedicated to transiting planet search took the lead in terms of number of detections. This technique requires a very accurate spectrograph which measures the periodic Doppler-Fizeau shift of the star's spectra as it moves around the star-planet barycenter. This wavelength shift  $\Delta\lambda$  is then translated into a measurement of the radial velocity  $v_r$  of the star towards the observer through  $\Delta\lambda/\lambda = -v_r/c$ . A Doppler precision of  $1 \text{ m.s}^{-1}$  typically corresponds to a stellar lines shift of 1/1000th of a CCD pixel.

In practice, the measured semi-amplitude  $K_*$  of the radial velocity of the host star  $v_r(t)$  can be expressed as

$$K_* [\text{cm s}^{-1}] = \frac{8.95}{\sqrt{1-e^2}} \frac{m \sin i}{M_\oplus} \left( \frac{M_* + m}{M_\odot} \right)^{-2/3} \left( \frac{P}{\text{yr}} \right)^{-1/3}, \quad (2)$$

where  $m$  is the planet mass,  $M_*$  is the star mass,  $M_\odot$  and  $M_\oplus$  are the Sun and Earth masses respectively,  $P$  is the orbital period expressed in years,  $e$  is the orbit

eccentricity and  $i$  is the orbit inclination. The detailed modeling of the radial velocity curve  $v_r(t)$  yields the measurement of  $P$ , as well as the eccentricity (distortion of  $v_r(t)$  relative to a sinusoidal curve), the longitude and time of the passage at the periastron, and of  $K_*$ . But as seen in the expression of  $K_*$ , the true mass of the planet  $m$  and the inclination  $i$  of the orbit remain degenerated. Hence only the planet minimum mass  $m \sin i$  is measured. Statistically, the probability that the inclination lies within  $i_1 < i < i_2$  is given by  $P = |\cos i_2 - \cos i_1|$ . It means that for example, there is 87% probability that the inclination of a given planet lies between thirty and ninety degrees (pure radial motion), or equivalently, a 87% probability that the true mass lies between the measured  $m \sin i$  and twice this value.

The reflex motion that Jupiter exerts on the Sun is about  $K_* \sim 12.5 \text{ m.s}^{-1}$ , while it drops to  $\sim 0.09 \text{ m.s}^{-1}$  when considering the pull of the Earth. These values have to be compared to the typical radial velocity precision achieved by the spectrographs: while in 1995, it was about  $10 \text{ m.s}^{-1}$ , in 1998 it improved to  $3 \text{ m.s}^{-1}$  and reached  $1 \text{ m.s}^{-1}$  in 2005 when the HARPS instrument mounted on the 3.6m telescope in La Silla (ESO Chile) was commissioned. These values may explain that there is so little literature speculating about the possibility of detecting exoplanets by measuring the radial velocity of stars before the first detection. The most likely reason is that the first generation of spectroscopes were far from being accurate enough and did not allow much hope. Indeed, measuring a Doppler shift is a very challenging task that requires high signal-to-noise ratio, high resolution, and large spectral coverage. The use of photographic plates and the approximate guiding at the spectrograph slit in the early 1970s limited the sensitivity to accuracies of about  $1 \text{ km.s}^{-1}$ . The advent of echelle spectrometers (using high diffraction orders) have revolutionized Doppler spectroscopy and allowed to reach the required precision to detect brown dwarfs and even exoplanets.

The formula giving  $K_*$  shows that more massive planets are easier to detect ( $K_*$  increases with  $m$ ), as well as shorter period (i.e. close-in) planets. Planets are also easier to find around low-mass stars than heavier stars. Furthermore, a planet must at least complete one full orbit in order to have its parameters constrained (although more orbits are usually needed to obtain good constraints). Hence when more data are collected with time, planets on larger orbits become detectable, in particular additional planets in already discovered systems.

Back in the early 1990s, and taking the Solar system as a reference, the short-orbit planets (Venus, Earth or Mars) were not massive enough to be detected, and the detection of Jupiter would require to wait for about 12 years. Early radial velocity searches were actually mainly focused on the characterization of the substellar and brown dwarf mass function by searching for companions of main sequence stars below one solar mass [12, 21], or were dedicated to establish improved radial velocity standards. As the accuracies improved toward  $10 - 20 \text{ m.s}^{-1}$ , the efforts increased and new observing programs started, leading to the monitoring of many more stars. At the end of the 1980s, many claims of exoplanet detections were retracted, which progressively introduce skepticism in the field. The case of  $\gamma$  Cep [6] is an instructive example: in 1988, variations in the residual velocities were clearly identified, but were attributed to stellar activity. In 2003, a reanalysis of the data obtained between 1981-2002 finally confirmed a planetary signal fifteen years later. Similarly in 1989, a 84-days periodic Doppler signal was detected around the star HD 114762, implying a companion of minimum mass of 11 Jupiter masses [20]. But because

of the ambiguity on the true mass since the orbital inclination was unknown, the data were misinterpreted as a probable brown dwarf signal, and only confirmed as a planet some years later.

In the climate of suspicion that dominates the mid-1990s, when M. Mayor et D. Queloz announced the detection of a possible planet around the solar-like star 51 Peg at the Observatoire de Haute Provence, stellar oscillations or non-radial pulsations were immediately invoked as possible sources of confusion in several publications. But the most striking fact about the discovery resided in the fact that the best model implied a minimum mass of about half of that of Jupiter, with an extraordinary orbital period of only 4.2 days (Fig. 4). For comparison, in the Solar system Jupiter has an orbital period of 12 years. While this very unexpected claim could have made an easy argument to refute the planetary interpretation, a number of events turned the situation around. First, the discovery was promptly confirmed by the Lick Observatory group, and second, this same group was also able to report two additional similar planets (large mass and very short orbits) around the Sun-like stars 70 Vir [22] and 47 UMa [5]. It then became quite clear that the main reason exoplanets were missed in the early years of monitoring is that the surveys were dedicated to detect planet with orbital periods larger than 10 years, where Jupiter analogs were thought to form. The discovery of these planets, called *hot Jupiters*, marked the beginning of a Doppler planet detection rush, and the birth of the field of extrasolar planet.

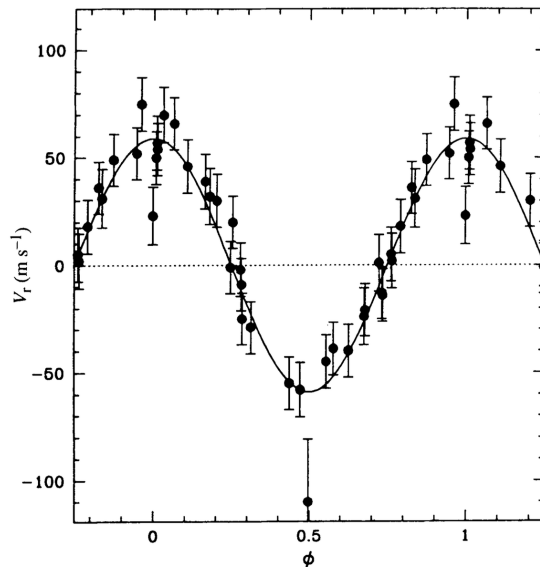


Figure 4: Radial velocity curve folded in phase of the 51 Peg b hot Jupiter. The model curve (solid line) accounts for a planet of half a Jupiter mass on a 4.2 days orbit (figure from [23]).

Nevertheless, the detection of significant eccentricity in many new exoplanet candidates did cast doubt again on the planetary interpretations, because many astronomers argued that planet should reside on circular orbits, in contrast with binary stars. Born in a gaseous disk, it was argued that planet eccentricities should be damped by the gas during the formation process. It is a well-known fact today



that planets can have large eccentricities, but the doubt was not left until the first transiting planet and multi-planetary systems were detected just before the turn of the 21st century.

Doppler spectroscopy plays an important role to confirm transiting exoplanets. New designs using near-infrared spectroscopy allows to monitor low-mass stars (red dwarfs), which account for up to 80% of the number of stars in the Milky Way. The smaller mass of the star makes it easier to detect low mass planets and at larger orbits. Observations at larger wavelengths are furthermore less sensitive to stellar activity that can mimic planetary signals.

### 2.3 Transit

When an exoplanet passes in front of its star, and given a suitable alignment between the planet, the star and the observer, the light from the host star is decreased by the transit of a planet across its disk, with the effect repeating at the orbital period (Fig. 5). The phenomenon is similar to the transit of Venus in front of the Sun as has been recently observed from Earth. The first exoplanet transit was detected in HD 209458 [17, 9], which was already known to harbor a planet thanks to Doppler spectroscopy. The duration of the transit was about 2.5 hours and had a depth of about 1.5%.

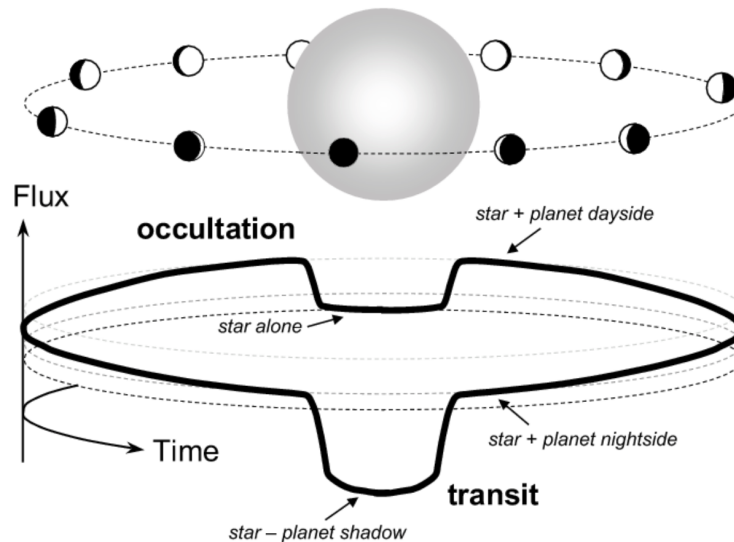


Figure 5: Transit curve with showing the primary eclipse (transit), the secondary eclipse (occultation) and the different phases.

The probability that a given exoplanet transits its host star is primarily a function of the inclination of the planetary orbit and of the stellar radius,

$$\mathcal{P}_{tr} = 0.0045 \left( \frac{\text{AU}}{a} \right) \left( \frac{R_{\star} + R_p}{R_{\odot}} \right) \left[ \frac{1 + e \cos(\pi/2 - \omega)}{1 - e^2} \right], \quad (3)$$

where  $\omega$  is the angle at which orbital periastron occurs ( $\omega = 90^\circ$  indicates transit), and  $e$  is the orbital eccentricity. A typical hot Jupiter around a solar-type star of

radius  $\sim R_{\text{Jup}}$  and period  $P \sim 3$  d has a transit probability  $\mathcal{P} \sim 10\%$ , a transit duration of  $\tau \sim 3$  hr and a photometric transit depth of  $d \sim 1\%$ . A super-Earth (few Earth masses) has typically  $\mathcal{P} \sim 2.5\%$ ,  $d \sim 0.1\%$ , and  $\tau \sim 6$  hr, while an Earth-like planet at 1 AU around a solar-type stars has  $\mathcal{P} \sim 0.5\%$ ,  $d \sim 0.01\%$ , and  $\tau \sim 15$  hr, which makes the detection very challenging. For nearly a decade, the community as a whole struggled to implement productive surveys. Expectations in terms of planet yield were largely overestimated. But after good strategies and new instruments were designed in the few years following the first discoveries, progress in transiting exoplanet detections went very fast. This is thanks to the increasing number of ground-based projects, such as the SuperWASP and HATNet surveys. Dozens of transiting planets with high-quality light curves have been gathered with accurate masses determined with precision Doppler velocity measurements. Thousands of additional transiting planetary candidates have been observed from space, with space missions CoRoT (CNES) and Kepler (NASA). Transit timing variations have progressed from a theoretical exercise to a practiced technique.

A serious challenge for wide-field surveys lies in the many ways transit can be affected by astrophysical false positives. Radial velocity measurements is then required (although other techniques are possible) to confirm the planetary nature of the signal. In that case, the exact mass and radius of the planet are measured, which yield the mean density. False positives may have different origin. Low mass stars and brown dwarfs overlap in size with giant planets, and have almost identical transit signatures to those of giant planets. Grazing eclipsing binaries (only a small fraction of the star's disk is eclipsed by the companion) can also provide an important source of confusion for low signal-to-noise light curves. When an eclipsing binary, either physically related or unrelated, shares the line of sight with the target star (flux received on the same pixel area), the total flux is increased and the apparent relative transit depth is consequently decreased, so that the transit depth appear smaller. False alarm probabilities are inferred to be dramatically lower for cases where multiple planets transit the same star. In this case, exoplanets can be confirmed on the grounds of transit signals only. In practice for the Kepler survey, the majority of the candidate planets cannot be confirmed by Doppler measurements, but about 800 planets were confirmed thanks to their multiple planet transits.

The flagship space missions Kepler and CoRoT have both exhibited excellent productivity, and a third mission, MOST, has provided photometric transit discoveries of several previously known planets. The Doppler technique, which was by far the most productive discovery method through 2006, is rapidly transitioning from a general survey mode to an intensive focus on low-mass planets and to the characterization transiting planets. The Kepler mission did provide hundreds of planet detections with mass determinations, as well as hundreds of multiple transiting planets orbiting a single host star, many of which are coplanar and rather crowded systems. The CoRoT satellite ceased active data gathering in late 2012, having substantially exceeded its three-year design life. In 2013, the Kepler satellite experienced a failure of a second reaction wheel, which brought its high-precision photometric monitoring program to an end, after four years of delivering high precision transit data.

New transit space missions have already been programmed for the next 10 years. NASA has selected the TESS mission that is scheduled for launch in 2017. It will monitor the all sky to locate transiting planets with periods of weeks to months, and sizes down to  $\sim 1 R_{\oplus}$  among a sample of  $5 \times 10^5$  stars including  $\sim 1000$  red

dwarfs. Another mission, the ESA CHEOPS satellite, is also scheduled for launch in 2017. It will selectively and intensively search for transits by already discovered high-precision Doppler planet candidates with radii in the range  $1 - 4 R_{\oplus}$ . It will also perform follow-up observations of interesting TESS candidates. Finally, the ESA PLATO mission will take over in 2025, with the objective to find and study a large number of extrasolar planetary systems, with emphasis on the properties of terrestrial planets in the habitable zone around solar-like stars. The satellite has also been designed to investigate seismic activity in stars, enabling the precise characterization of the planet host star, including its age.

## 2.4 Gravitational microlensing

In 1936, Einstein derived the equations of the bending of light rays originating from a background star when passing in the vicinity of a foreground star, what is called today gravitational microlensing. At the time the article came out, however, observational facilities were not developed enough yet to seriously consider detecting a microlensing effect. Einstein himself concluded: “there is no great chance of observing this phenomenon”. But 50 years after Einstein’s publication, the astrophysicist Bohdan Paczyński [24] revisited the basic ideas of microlensing observations, in a seminal article published in 1986. The original idea of the paper was to propose a new method to detect hypothetical dark, compact, massive halo objects (MACHOs) as a possible form of dark matter in the Milky Way. A number of observational searches with line of sights towards the Large and Small Magellanic Clouds and the Galactic center in particular were subsequently initiated beginning of the 1990s: MACHO (Massive Compact Halo Object), EROS (Experience pour la Recherche d’Objets Sombres) and OGLE (Optical Gravitational Lensing Experiment). In 1993, the first stellar microlensing events were detected independently by the MACHO and EROS collaborations. These detections mark the birth of microlensing as an observational technique. About 3000 events are now detected every year, which provide unique astrophysical informations in several fields of research in astronomy and astrophysics.

Compared to other planet detection methods, microlensing detections bring unique information on planetary populations that justified the strong and steady efforts to make the technique work. While most planets detected with other methods are detected close to their stars, prime targets of microlensing are planets located beyond the snow line of their stars, where ices can start to form. A full understanding of the demographics of extrasolar planet in the Galaxy thus relies on the combination of the different observational techniques. During decade 2003-13, the most important microlensing results include the discovery of the first ever cool super-Earth planet (2005), the discovery of Jupiter-mass free-floating planets (2012), and first constraints on the planetary mass function for a wide range of masses and orbital distances (2012). At the end of a decade filled with discoveries, microlensing observations find that, on average, every Milky Way star has a planet, and that planets around stars are the rule rather than the exception.

Gravitational microlensing describes the bending of light from a background source star due to the gravitational field of a compact object crossing the observer-source line-of-sight, and acting as a lens. The geometry of the problem is shown in Fig. 6. Light rays passing in the vicinity of the microlens will be bent by gravity by

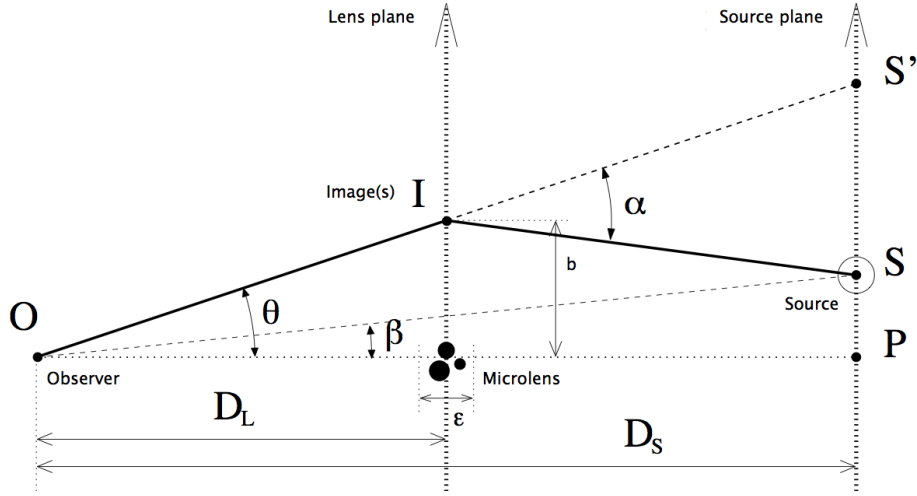


Figure 6: Geometry of a microlensing event. The source is located in the background, and is lensed by a foreground lensing star or planetary system (figure from [7]).

an angle  $\hat{\alpha} \ll 2\pi$  given by

$$\hat{\alpha} = \frac{4GM}{c^2} \frac{1}{|b|}, \quad (4)$$

where  $|b|$  is the closest approach distance of the light ray from the lens,  $M$  is the total mass of the lens,  $c$  the speed of light and  $G$  the gravitational constant. In general, multiple images of the source are produced, but in the ideal case of a single point-mass lens perfectly aligned with a point-source, the image of the source is a circle of angular radius  $\theta_E$ , or angular Einstein ring radius,

$$\theta_E = (\kappa M \pi_{\text{rel}})^{1/2}, \quad (5)$$

where  $\pi_{\text{rel}} \equiv \text{AU}/D_L - \text{AU}/D_S$  is the relative lens-source parallax,  $D_L$  and  $D_S$  are the observer-lens and observer-source distances,  $\kappa \simeq 4G/c^2 \text{AU} \simeq 8.144 \text{mas}/M_\odot$ ;  $M$  is expressed in  $M_\odot$  units and  $\pi_{\text{rel}}$  in mas. Numerically,

$$\theta_E \simeq 0.638 \left( \frac{M}{0.5 M_\odot} \right)^{1/2} \left( \frac{\pi_{\text{rel}}}{0.1 \text{mas}} \right)^{1/2} \text{mas}. \quad (6)$$

With typical values of  $\theta_E$  of order of a fraction of a mas, it is impossible with classical telescopes to resolve the individual images of the source, since a fraction of an arcsecond is the usual resolution limit. But the images of the source produced by the microlens are distorted and magnified (images of the source have larger total area than the original, not lensed one), so that the total flux appear amplified during a microlensing event. In the simple case of an isolated microlens, the total magnification is given by

$$\mu = \frac{u^2 + 2}{u\sqrt{u^2 + 4}}, \quad (7)$$

where  $u$  is the projected separation between the source and the lens in  $\theta_E$  units. Since the source and the lens move with time,  $\mu$  is a function of time. For a lens source

rectilinear motion, such single-lens temporal magnification curves have a typical bell-shape aspect, with maximum magnification at peak that can reach many hundreds if the alignment is particularly good. The typical light curve of a planetary event is shown in Fig. 7.

After the microlensing pioneer times of decade 1993-2003, spent in improving the observing strategy and the instruments, the first microlensing exoplanet, a  $2.6 M_{\text{Jup}}$  planet, was detected in event OGLE-2003-BLG-235/MOA-2003-BLG-53Lb. A milestone discovery was OGLE 2005-BLG-390 [4], the very first cool super-Earth with a mass of  $5.5 M_{\oplus}$  and semi-major axis of 2.6 AU, and discovered in 2005. Massive Jovian planets around low-mass red dwarfs have been discovered by microlensing, as OGLE-2005-BLG-071 and MOA-2009-BLG-387. The existence of such planets challenges the core accretion theory of planet formation, since it predicts that massive, Jovian planets should be rare around M dwarfs. Multi-planet systems have been discovered too, OGLE-2006-BLG-109 and OGLE-2012-BLG-0026. The first system is actually a scaled-down model of our solar system, with two planets analogs as Jupiter and Saturn, but of lower masses. Microlensing has discovered a population of free-floating planets [27], which may be as frequent as stars in the Milky Way. These events are of very short timescale, less than two days.

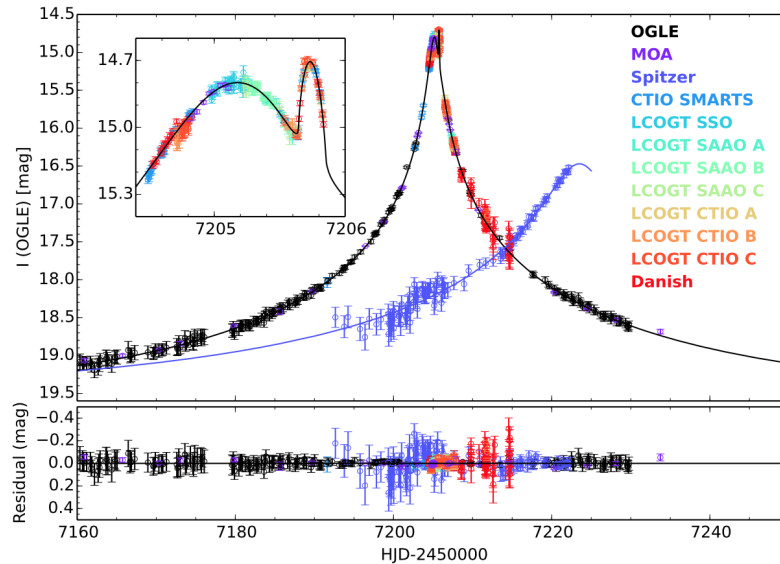


Figure 7: Light curve of OGLE-2015-BLG-0966, with combined data from 10 ground-based telescopes (data fitting the black solid line model). The violet curve is a light curve obtained with the Spitzer satellite. The shift between the two light curve provide important constraints on the lens-source parallax and so on the microlens physical parameters (figure from [26]).

With 700 alerts per year in 2009 to about 2500 in 2011, the OGLE collaboration has already quadrupled its number of alerted microlensing events. New generations of robotic telescopes equipped with wide-field cameras (KMNET, LCOGT) are joining the microlensing networks, complementing earlier-generations telescopes (OGLE IV, MOA II, PLANET,  $\mu$ FUN, RoboNET, MiNDSTEp) together with an increasing number of amateur telescopes. The growing number of light curves requires the implementation of high performance and automated modeling tools working in real

time.

Microensing observations from space have been carried out with the Rosetta spacecraft to confirm the planetary nature of microlensing candidates in 2004. Since 2014, the Spitzer satellite observes microlensing events to measure the lens-source parallax, with spectacular results (see Fig. 7). Specific space-based microlensing programs have been proposed onboard the Euclid satellite (ESA, launch in 2020, additional science) and WFIRST (NASA, planning phase). Simulations show that for such space-based microlensing missions a great number of planets, including Earth-like planets, should be detected in a few months, and unprecedented constraints on the planetary mass function down to the mass of the Earth should be obtained.

## 2.5 Imaging

Probably the most natural observation technique in astronomy is to make an image of the object one wants to study. In exoplanet research, this technique is called direct imaging (in contrast with previous methods which relied on indirect effects). Imaging an exoplanet is not an easy task, though: exoplanets like those we know in our Solar system are billions of times fainter than their host stars and situated at extremely close angular separations from their host star. Current imaging techniques can detect an exoplanet  $10^5$  times fainter than its host star, at about 1 arcsecond separation. Although this is already a technical prowess, it is still far from what is required to detect a planet like Jupiter around another Sun.

The direct imaging challenge is to separate the light from the planet to the light from the star, which is diffracted by the telescope. The instruments themselves are designed to block or annulate the light from the star, while the post-observation softwares are designed to distinguish between diffraction features due to the planet or to the star. Coronagraphs are the central piece of direct imaging instruments. The basic principle of imaging has been invented by Lyot in 1939: the light from the star is blocked on the optical axis by a focal plane mask (called Lyot stop), while in the pupil-plane located after, another mask blocks the light diffracted off-axis, in order to remove the starlight. Since the exoplanet is not located on the optical axis but makes a small angle with it, the light from it is not blocked by the Lyot stop and will consequently appear as a classical image. Apodizers are designed to modify the transmission of the telescope so that power of the sidelobes (off-axis) of the star light is minimum, to increase the contrast between this residual light from that of the planet (Fig. 8).

In practice, many optical designs have been proposed and implemented to specifically search for exoplanets, usually employing cutting edge technology. Direct imaging also requires adaptive-optic mirrors to correct for atmospheric turbulence beforehand. In fact, atmospheric turbulence is responsible for polluting the image with a halo of speckles that rapidly evolve, and mask planetary signals. Today, the best coronagraphs can remove diffraction down to the level of  $10^{-10}$  at separations larger than  $2 - 4\lambda/D$ .

Direct imaging is primarily sensitive to massive planets at wide orbits from their parent stars (greater than about 5 AU). The main (and still only) targets of this method are young exoplanets, which emit infrared light from the heat they accumulated during their formation phase and subsequently release it for a few tens million years (to be compared with e.g. the lifetime of the Sun, about 10 billion

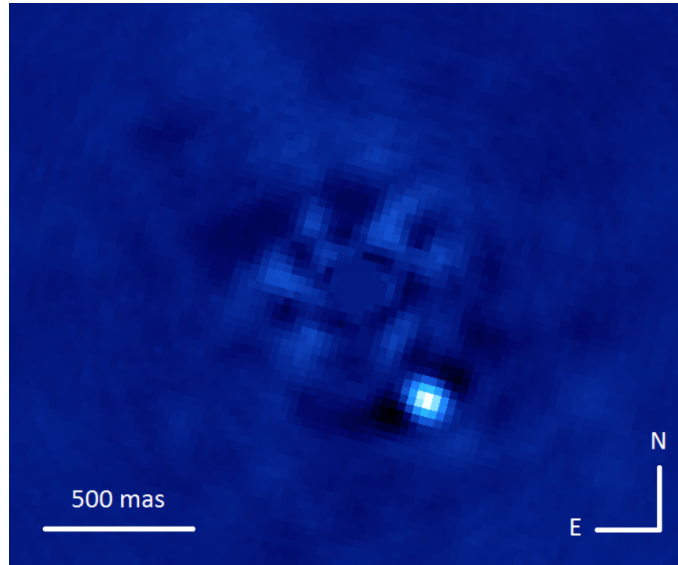


Figure 8: Imaging of the planetary system  $\beta$  Pic using the AGPM coronagraph on VLT/NACO (image in linear flux scale). The giant planet visible on the image is at 8-9 AU from the star. The technique allows to rule out the presence of additional giant companions down to orbits of 2 AU only (figure from [1]).

years). The effective temperature of these young planets can reach up to 2000 K (for Jupiter today, this temperature is about 150 K). One of the main difficulty is to derive the mass from the planet's luminosity, since the latter is the only observable. Evolutionary models of the temperature as a function of age have to be used, which introduces a degree of uncertainty in the determination of the planetary masses.

In 2004, the first major discovery was that of a giant planet of 5 times the mass of Jupiter in orbit around a brown dwarf aged of about 8 million years [10]. Several detections followed, amongst them the detection of young, multiple planetary systems. In cases when the planet is sufficiently separated from its host star, direct spectroscopy observations can be performed. Planets observed this way have low gravity (as expected from the fact they still hot and slowly cooling down), and distinct atmospheric structures from brown dwarfs. In very favorable cases, individual spectral lines such as CO lines can be directly observed. These are important pieces of information when trying to understand the formation mechanisms of super-giant planets vs. brown dwarfs. When possible, direct imaging in the optical, although much more challenging since the planet-star contrast is much higher (the maximum black body emission of the planet is in the infrared, and lies in the Rayleigh-Jeans wing of the star's black body), provide important information on the albedo of the planet, and on its cloud cover.

The current approach is to develop new direct imaging instruments to specifically search for exoplanets. An adaptive optics system using 2000 actuators has been mounted on the Subaru telescope (Hawaii) to serve as a testbed for future technologies. Two instruments have been recently commissioned and have obtained first very detailed and highly contrasted images: the Gemini Planet Finder, and the SPHERE instrument at the Very Large Telescope (ESO), both located in Chile. The upcoming European Extremely Large Telescope (E-ELT), the future largest optical

and near-infrared 39 m telescope is scheduled to take its first image in 2024, and should be able to reach planet-star separations of only 0.2 arcsecond. Imaging space missions are not planned, but instruments are developed onboard JWST (future space telescope in replacement of Hubble, launch planned in 2018) and prototype chronographs are studied for the future WFIRST mission (NASA).

## 2.6 Astrometry

Astrometry consists in measuring the position and motion of objects in the plane of the sky. It is probably the oldest branch of astronomy. Historically, many retracted discovery were announced starting at the end of the 1930s, when photographic plates became of good enough quality. One famous case is Barnard's star, for which two planetary-mass bodies of 0.7 and 0.5 Jupiter masses with periods of 12 and 20 years were proposed, and discussed many times for about 30 years. However, the sensitivity was much too low for a planet to be detected at all at that time, and even today this method has not produced any confirmed exoplanet. Nevertheless, the ESA satellite mission Gaia should report many detections in a very near future.

An astrometric orbit corresponds to the barycentric motion of a star caused by an invisible companion. This motion follows Kepler's laws, and astrometric measurements determine the value of  $m^3/(M_* + m)^2$ , where  $M_*$  is the host star mass and  $m$  the companion mass. Astrometry is applicable to planet searches around nearby stars of various masses and ages, with benefits for the study of the planet mass function of long-period planets, and of planets around active stars.

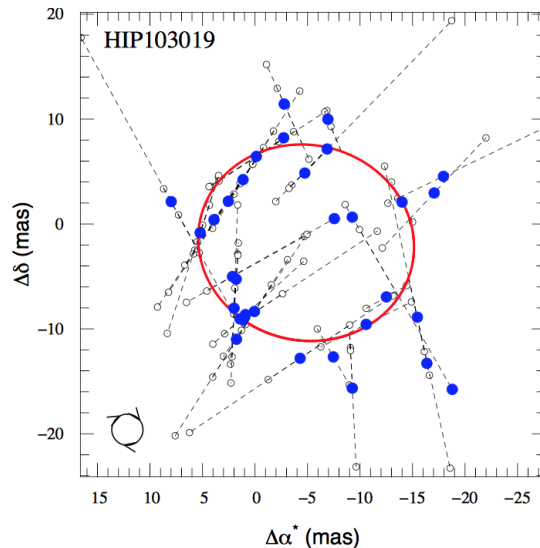


Figure 9: Determination of the astrometric orbit of the companion of star first detected via Doppler spectroscopy. The solid red line shows the orbital solution and open circles mark the individual Hipparcos astrometric measurements (figure from [25]).

At the time being, astrometry is used in combination with Doppler spectroscopy to refine the planet parameters (Fig. 9). In fact, only five out of seven orbital parameters are constrained by radial velocity measurements alone, and the two remaining



parameters, the inclination  $i$  and the longitude of the ascending node  $\Omega$  can be determined by measuring the astrometric orbit. The ESA satellite Hipparcos yielded mass upper limits on the mass of several planets, thus putting strong constraints on the inclinations of the planetary orbits. In some rare cases, it revealed that brown dwarfs or stellar companions had been mistaken for planets. The Hubble space telescope was also used for this purpose.

## 2.7 Other detection channels

There are many other ways to detect exoplanets, like eclipsing binary timing, radio astrometry, transit time variation, X rays emission, destabilization of debris disks... but we cannot expect these methods to contribute to the bulk of exoplanet detections. The detection of radio emission due to the interaction of the star and planet magnetospheres is an interesting possibility using imaging or astrometry. Since the first exoplanet discoveries, radio detections have been attempted numerous times, with various telescopes and at different frequencies. Although there are significant uncertainties in predicting which exoplanets are most likely to be the strongest radio emitters, until now searches have focused on the short-period planets.

## 3 A wealth of possible worlds

Exoplanet search campaigns have discovered a great variety of possible planets in terms of mass, orbital parameters such as eccentricity and inclination, mean densities, composition, size, or atmospheric structure to quote a few aspects. Planetary systems are shaped by formation mechanisms, different types of orbital migration, multiple body gravitational interaction, collisions, ejection of small bodies or ejection of giant planets, resonance between orbital parameters in multiple planetary systems, and many other subtle effects.

For example, the growth of planetary embryos can follow an oligarchic growth, which assumes that embryos grow from a swarm of kilometer-size planetesimals, while a more recent scenario states that the accretion of pebbles can grow an Earth-mass planet directly from cm-sized bodies in favorable conditions. These scenarios do not build up the same kinds of planets. Super-Earth planets (from 1 to 10  $M_{\oplus}$ ) can form either *in situ* by accretion of locally available material in massive disks, but they can also form at larger orbital distances and then migrate inward by interactions with the gaseous disk. The planets formed following the first recipe might not be able to capture an atmosphere, and they would all be rocky, while in the second case for the same mass, they could sustain a massive atmosphere.

The orbital migration of planets is usually an inward migration, but in some conditions it can be outward. The comparison of the number of planets located beyond or within the snow line provides important information on the efficiency of migration mechanisms. Furthermore, there are other types of migration that do not need to be gas-driven. Planet-planet scattering is another option, and migration can occur in this case after the dispersal of the gas a few million years after the birth of the star.

Many exoplanets have large eccentricities, which was unexpected. The main stages of planet formation occur in the gaseous disk, and the presence of gas very efficiently damps eccentricities and orbital inclinations, through viscous drag between

the solid bodies (planetesimals or planet embryos) and the gas. The post-gaseous dynamical evolution of exo-planetary systems appears to be much more complex than was suggested by the coplanar and almost circular orbits of the planets around the Sun.

Giant planets can grow from solid planetary cores formed by accretion, in other words can use a newly-formed terrestrial planet as a core to later accrete a significant amount of gas. In this case, the planet is expected to include a fraction of solids (dust) substantially higher than that of the proto-planetary disk. Another scenario proposes the direct formation of a giant planet by gravitational instability in the proto-planetary disk, provided that the disk is massive enough. Such planets would form at large orbital distances, where the temperature is cold enough to ease gravitational collapse.

At greater masses, super-giant planets have been found to overlap with the range of masses historically attributed to brown dwarfs ( $13 - 74 M_J$ ). The latter are stars that could not ignite hydrogen in their core to become real stars, but still could burn deuterium for a few million years. It is not clear which have been formed by which mechanisms. Although the detection of these objects is far more easier than the detection of terrestrial planets, there are still very few discoveries because objects in this range of masses are intrinsically rare around stars – it is called the brown dwarf desert. More generally, the frequency of companions drops with increasing mass, and the frequency of super-giant planets and brown dwarfs companions to stars is estimated to be as low as 1%.

Some hot Jupiters have been found to be exaggeratedly inflated: although of Jupiter mass, some can have sizes of several times Jupiter's radius. The origin of these large radii is still unclear, but the basic reason is the atmosphere do not release its energy and increases its volume. It may be that the molecules of the upper atmosphere are ionized by the strong irradiation due to the proximity of the star, which produces electric conduction and results in heating through ohmic resistivity. Another hypothesis is the presence of clouds, which increase the opacity of the atmosphere.

Early discoveries have shown that exoplanets can be found in orbit around one of the components of a wide-separation binary star. While the planets are always located relatively far from destabilizing resonances, the stability of the proto-planetary disks can be questioned in some cases. More recently in 2011, planets orbiting close binary systems have been discovered [11]. In this case, the exoplanet orbits the pair of stars, and is called circum-binary exoplanet.

For a subset of objects, it has been possible to measure a Rossiter-McLaughlin effect, which results from the fact that a transiting planet blocks sequentially Doppler-shifted area of the star due to its rotation. The angle between the spin of the star and the orbit of the planet can then be measured through analysis of the radial velocity curve. In a normal case, this angle is null, as it is the case in the Solar system. But several exoplanets do exhibit a spin-orbit misalignment, which probably results from early dynamical interactions with other planets in the formation phase.

Another recent discovery is that in the super-Earth mass regime, there are not only heavier version of rocky planets like the Earth, but also planets with massive atmospheric envelopes of hydrogen and helium (Fig. 10). Intermediate radius could indicate ocean planets with atmospheres saturated of water vapor.

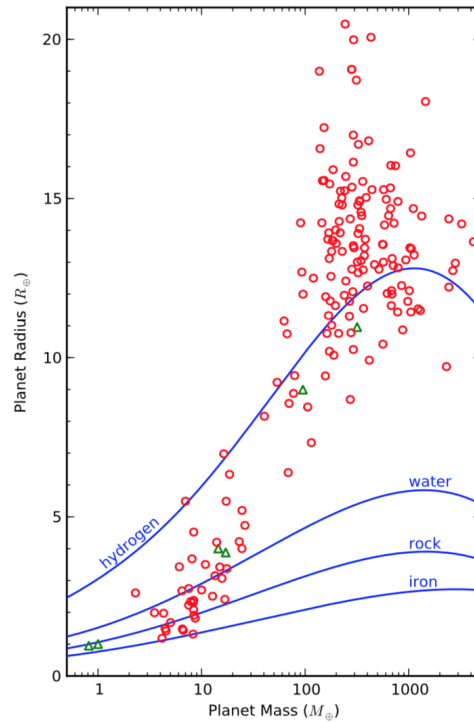


Figure 10: Masses and radii of exoplanets (red dots). The blue lines are mass-radius relationships for planets with pure hydrogen, water, rock or iron (figure from [13]).

Exoplanets not related to any star are called free-floating planets. They have been discovered via direct imaging and microlensing. While for the largest objects it may be that they formed directly by gravitational instability, for Jupiter-mass objects it is very likely that they were ejected from their planetary system after the gas was dispersed from the proto-planetary disk. If the system had formed two giant planets located too close to each other, gravitational interaction may result in the ejection of one of the planet, with the second planet moved to an eccentric orbit. Indeed, many extrasolar planets have rather large eccentricities, although there are many possible origins for that.

Precise spectroscopy of transiting planets have revealed the presence of molecules in the atmosphere of giant planets, in particular water vapor [28]. In other hot giant planets, spectroscopy resulted in flat spectra which could result from a thick cloud cover or haze in the planetary atmosphere.

Phases of hot Jupiter planets can be sometimes observed (Fig. 5) and the wind speed of equatorial jets measured at the surface of hot Jupiters via the displacement of the hottest point on the planet's surface.

Finally, families of comets have been found around stars harboring planets [19], as it is the case in our Solar system.

#### 4 Rule rather than exception: more exoplanets than stars in the Milky Way

Statistical studies aim at understanding the planetary populations and at constraining their frequency, beyond the observational biases which confuse the picture. For

example, naively reading Fig. 2 would suggest that hot Jupiters are very numerous (many planets at large masses and very short orbit), but in reality they account for less than a few percents of the full population. Super-Earths on contrary are not very often detected, but they actually form the largest population of exoplanets known today — keeping in mind we don't know yet how frequent are Earth-like planets. We describe below a statistical study based on microlensing data.

Giant planets located at a few AUs, like Jupiter in the Solar System, were the prime targets of the first microlensing campaigns starting in 1995. The large caustic structures implied a planet detection efficiency as high as 100% for well-covered events observed at high magnification. Because of this very high detection efficiency, many giant planets should have been detected quickly, but no planets were found yet after the first five years of observations. While part of the negative result has roots the chosen observing strategy, after a few years it became clear that giant planets at large orbital distances were intrinsically rare. The hunt for extrasolar planets through microlensing revealed itself to be more challenging than initially thought. Early statistical estimations using microlensing 1995-99 data [15] led to first significant upper limits on the abundance of giant planets around red dwarfs: less than 1/3 of the lens stars had Jupiter-mass companions, while less than 2/3 of the lenses had Saturn-mass companions in the orbital range 1.5 – 4 AU.

After 2005, the  $\mu$ FUN microlensing collaboration took advantage of a growing community of amateur astronomers observing microlensing events to set up a very reactive observing strategy dedicated to detect and characterize high-magnification events. During the 4 seasons 2005-08, high-magnification events were monitored as intensively as possible, independently of any evidence of a light curve anomaly. This strategy turned out to be very efficient: half of the events monitored were planetary events. In order to estimate the planet frequency from these high-magnification events, an unbiased sample of 13 high-magnification events with peak magnification greater than 200 was selected. A point on the planetary mass function could be estimated [16],  $f = 0.36 \pm 0.15 \text{ dex}^{-2}$  per  $\log q \times \log d$ . This result was consistent with Doppler estimates when considering that Doppler hosts are G dwarfs rather than M dwarfs, and when planetary systems are scaled to the location of their snow line.

With a database rich with about 15 years of data obtained with a world-wide network of telescopes, in 2010 the PLANET collaboration had a much higher sensitivity to low-mass planets than previous studies. The analysis was based on 1995-2010 PLANET data alerted by OGLE, using detections and non-detections [8]. In order to be combined in a meaningful statistical analysis, two critical conditions were required. First, the observing strategy should be well understood and keep homogeneous for the whole sample of events, which required that the event selection and sampling rate was chosen regardless of whether the lens harbored a planet or not. Secondly, the detections should result from exactly the same strategy than for the non-detections. It resulted from a detailed study of the statistical properties of the microlensing events that only a sub-sample of six years of data, 2002-07, satisfied these requirements. In fact, when starting its new operations in 2002, OGLE III dramatically increased its number of alerts compared to OGLE II (389 in 2002 vs. 78 alerts in 2000), which had a strong impact on the PLANET strategy. After 2007, a very open collaboration between the different microlensing teams again re-

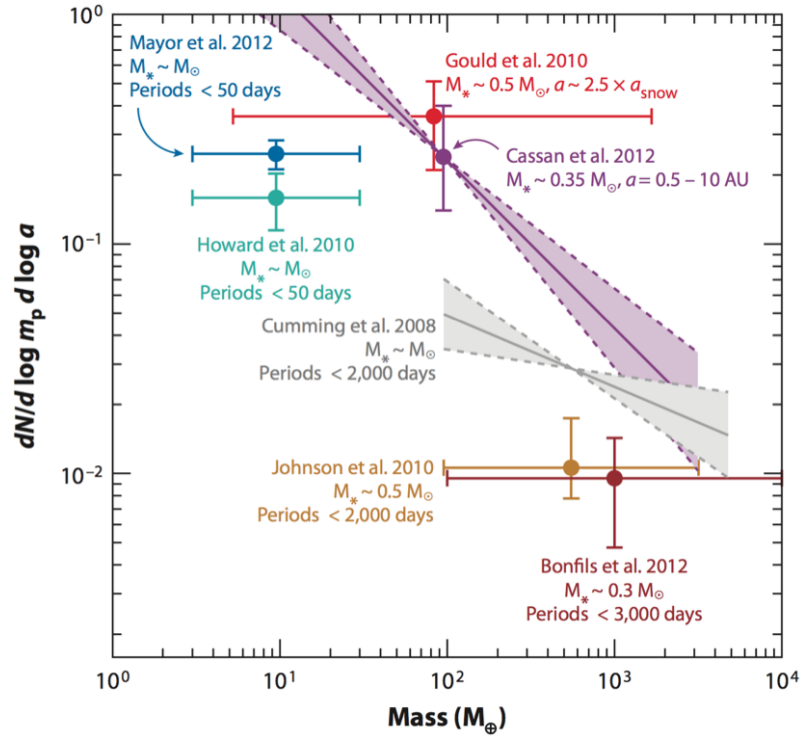


Figure 11: Various planetary mass function constraints from different analysis using microlensing and radial velocity data (figure from [14]).

sulted in a dramatic change in the observing strategy. During 2002-07, PLANET monitored around 10-16% of all OGLE alerts. A power-law planetary mass function was derived from this analysis,

$$f = 10^{-0.62 \pm 0.22} \left( \frac{M}{95 M_E} \right)^{-0.73 \pm 0.17}, \quad (8)$$

centered on Saturn's mass. The microlensing result implied that  $17_{-9}^{+6}\%$  (1/6) of stars host Jupiter-mass planets ( $0.3\text{-}10 M_J$ ), while cool Neptunes ( $10\text{-}30 M_E$ ) and super-Earths ( $5\text{-}10 M_E$ ) are even more common, with respective abundances per star of  $52_{-29}^{+22}\%$  (1/2) and  $62_{-37}^{+35}\%$  (2/3). Planets around Milky Way stars are the rule rather than the exception.

Different planetary mass function estimations from microlensing and other detection techniques are shown in Fig. 11. It is important to note that they are not directly comparable, because the methods don't have the same sensitivity, and because the planets may not orbit the same types of stars.

## 5 Epilogue

In about two decades, we progressed from the observation of one to several hundreds of planetary systems. Many complementary techniques have led to the discovery of an astonishing diversity of foreign worlds. There are one to two hundred billion stars in the Milky Way, and even more exoplanets... how many options does it represent

for the apparition of extraterrestrial life? The field of exoplanet research has open the door, but nobody knows yet what stands behind.

## References

- [1] Absil, O., Milli, J., Mawet, D., Lagrange, A.-M., Girard, J., Chauvin, G., Boccaletti, A., Delacroix, C., and Surdej, J.: Searching for companions down to 2 AU from  $\beta$  Pictoris using the L'-band AGPM coronagraph on VLT/NACO. *Astron. Astrophys.* **559**, L12 (2013).
- [2] Backer, D. C., Foster, R. S., and Sallmen, S.: A second companion of the millisecond pulsar 1620 - 26. *Nature* **365**, 817–819 (1993).
- [3] Bailes, M., Lyne, A. G., and Shemar, S. L.: A planet orbiting the neutron star PSR1829 - 10. *Nature* **352**, 311–313 (1991).
- [4] Beaulieu, J.-P., Bennett, D. P., Fouqué, P., Williams, A., Dominik, M., Jørgensen, U. G., Kubas, D., Cassan, A., Coutures, C., Greenhill, J., Hill, K., Menzies, J., Sackett, P. D., Albrow, M., Brilliant, S., Caldwell, J. A. R., Calitz, J. J., Cook, K. H., Corrales, E., Desort, M., Dieters, S., Dominis, D., Donatowicz, J., Hoffman, M., Kane, S., Marquette, J.-B., Martin, R., Meintjes, P., Pollard, K., Sahu, K., Vinter, C., Wambsganss, J., Woller, K., Horne, K., Steele, I., Bramich, D. M., Burgdorf, M., Snodgrass, C., Bode, M., Udalski, A., Szymański, M. K., Kubiak, M., Więckowski, T., Pietrzyński, G., Soszyński, I., Szewczyk, O., Wyrzykowski, Ł., Paczyński, B., Abe, F., Bond, I. A., Britton, T. R., Gilmore, A. C., Hearnshaw, J. B., Itow, Y., Kamiya, K., Kilmartin, P. M., Korpela, A. V., Masuda, K., Matsubara, Y., Motomura, M., Muraki, Y., Nakamura, S., Okada, C., Ohnishi, K., Rattenbury, N. J., Sako, T., Sato, S., Sasaki, M., Sekiguchi, T., Sullivan, D. J., Tristram, P. J., Yock, P. C. M., and Yoshioka, T.: Discovery of a cool planet of 5.5 Earth masses through gravitational microlensing. *Nature* **439**, 437–440 (2006).
- [5] Butler, R. P., and Marcy, G. W.: A Planet Orbiting 47 Ursae Majoris. *Astrophys. J.* **464**, L153 (1996).
- [6] Campbell, B., Walker, G. A. H., and Yang, S.: A search for substellar companions to solar-type stars. *Astrophys. J.* **331**, 902–921 (1988).
- [7] Cassan, A.: Extrasolar planets detections and statistics through gravitational microlensing. Master's thesis, Sorbonne Universités, UPMC Univ Paris 06, CNRS UMR 7095, Institut d'Astrophysique de Paris, F-75014, Paris, France <EMAIL>cassan@iap.fr</EMAIL>, October 2014.
- [8] Cassan, A., Kubas, D., Beaulieu, J.-P., Dominik, M., Horne, K., Greenhill, J., Wambsganss, J., Menzies, J., Williams, A., Jørgensen, U. G., Udalski, A., Bennett, D. P., Albrow, M. D., Batista, V., Brilliant, S., Caldwell, J. A. R., Cole, A., Coutures, C., Cook, K. H., Dieters, S., Prester, D. D., Donatowicz, J., Fouqué, P., Hill, K., Kains, N., Kane, S., Marquette, J.-B., Martin, R., Pollard, K. R., Sahu, K. C., Vinter, C., Warren, D., Watson, B., Zub, M., Sumi, T., Szymański, M. K., Kubiak, M., Poleski, R., Soszynski, I., Ulaczyk, K., Pietrzyński, G., and Wyrzykowski, Ł.: One or more bound planets per Milky Way star from microlensing observations. *Nature* **481**, 167–169 (2012).

- [9] Charbonneau, D., Brown, T. M., Latham, D. W., and Mayor, M.: Detection of Planetary Transits Across a Sun-like Star. *Astrophys. J.* **529**, L45–L48 (2000).
- [10] Chauvin, G., Lagrange, A.-M., Dumas, C., Zuckerman, B., Mouillet, D., Song, I., Beuzit, J.-L., and Lowrance, P.: A giant planet candidate near a young brown dwarf. Direct VLT/NACO observations using IR wavefront sensing. *Astron. Astrophys.* **425**, L29–L32 (2004).
- [11] Doyle, L. R., Carter, J. A., Fabrycky, D. C., Slawson, R. W., Howell, S. B., Winn, J. N., Orosz, J. A., Prcaronsa, A., Welsh, W. F., Quinn, S. N., Latham, D., Torres, G., Buchhave, L. A., Marcy, G. W., Fortney, J. J., Shporer, A., Ford, E. B., Lissauer, J. J., Ragozzine, D., Rucker, M., Batalha, N., Jenkins, J. M., Borucki, W. J., Koch, D., Middour, C. K., Hall, J. R., McCauliff, S., Fanelli, M. N., Quintana, E. V., Holman, M. J., Caldwell, D. A., Still, M., Stefanik, R. P., Brown, W. R., Esquerdo, G. A., Tang, S., Furesz, G., Geary, J. C., Berlind, P., Calkins, M. L., Short, D. R., Steffen, J. H., Sasselov, D., Dunham, E. W., Cochran, W. D., Boss, A., Haas, M. R., Buzasi, D., and Fischer, D.: Kepler-16: A Transiting Circumbinary Planet. *Science* **333**, 1602 (2011).
- [12] Duquennoy, A., and Mayor, M.: Multiplicity among solar-type stars in the solar neighbourhood. II - Distribution of the orbital elements in an unbiased sample. *Astron. Astrophys.* **248**, 485–524 (1991).
- [13] Fischer, D. A., Howard, A. W., Laughlin, G. P., Macintosh, B., Mahadevan, S., Sahlmann, J., and Yee, J. C.: Exoplanet Detection Techniques. *Protostars and Planets VI*, pages 715–737 (2014).
- [14] Gaudi, B. S.: Microlensing Surveys for Exoplanets. *ARA&A* **50**, 411–453 (2012).
- [15] Gaudi, B. S., et al: Microlensing constraints on the frequency of jupiter-mass companions: Analysis of 5 years of planet photometry. *Astrophys. J.* **566**, 463–499 (2002).
- [16] Gould, A., Dong, S., Gaudi, B. S., Udalski, A., Bond, I. A., Greenhill, J., Street, R. A., Dominik, M., Sumi, T., Szymański, M. K., Han, C., Allen, W., Bolt, G., Bos, M., Christie, G. W., DePoy, D. L., Drummond, J., Eastman, J. D., Gal-Yam, A., Higgins, D., Janczak, J., Kaspi, S., Kozłowski, S., Lee, C.-U., Mallia, F., Maury, A., Maoz, D., McCormick, J., Monard, L. A. G., Moorhouse, D., Morgan, N., Natusch, T., Ofek, E. O., Park, B.-G., Pogge, R. W., Polishook, D., Santallo, R., Shporer, A., Spector, O., Thornley, G., Yee, J. C.,  $\mu$ FUN Collaboration, Kubiak, M., Pietrzyński, G., Soszyński, I., Szewczyk, O., Wyrzykowski, Ł., Ulaczyk, K., Poleski, R., OGLE Collaboration, Abe, F., Bennett, D. P., Botzler, C. S., Douchin, D., Freeman, M., Fukui, A., Furusawa, K., Hearnshaw, J. B., Hosaka, S., Itow, Y., Kamiya, K., Kilmartin, P. M., Korpela, A., Lin, W., Ling, C. H., Makita, S., Masuda, K., Matsubara, Y., Miyake, N., Muraki, Y., Nagaya, M., Nishimoto, K., Ohnishi, K., Okumura, T., Perrott, Y. C., Philpott, L., Rattenbury, N., Saito, T., Sako, T., Sullivan, D. J., Sweatman, W. L., Tristram, P. J., von Seggern, E., Yock, P. C. M., MOA Collaboration, M. Albrow, Batista, V., Beaulieu, J. P., Brilliant, S., Caldwell, J., Calitz, J. J., Cassan, A., Cole, A., Cook, K., Coutures, C., Dieters, S., Dominis Prester, D., Donatowicz, J., Fouqué, P., Hill, K., Hoffman, M., Jablonski, F., Kane, S. R., Kains, N.,

- Kubas, D., Marquette, J.-B., Martin, R., Martioli, E., Meintjes, P., Menzies, J., Pedretti, E., Pollard, K., Sahu, K. C., Vinter, C., Wambsganss, J., Watson, R., Williams, A., Zub, M., PLANET Collaboration, Allan, A., Bode, M. F., Bramich, D. M., Burgdorf, M. J., Clay, N., Fraser, S., Hawkins, E., Horne, K., Kerins, E., Lister, T. A., Mottram, C., Saunders, E. S., Snodgrass, C., Steele, I. A., Tsapras, Y., RoboNet Collaboration, Jørgensen, U. G., Anguita, T., Bozza, V., Calchi Novati, S., Harpsøe, K., Hinse, T. C., Hundertmark, M., Kjærgaard, P., Liebig, C., Mancini, L., Masi, G., Mathiasen, M., Rahvar, S., Ricci, D., Scarpetta, G., Southworth, J., Surdej, J., Thöne, C. C., and MiND-STEP Consortium: Frequency of Solar-like Systems and of Ice and Gas Giants Beyond the Snow Line from High-magnification Microlensing Events in 2005–2008. *Astrophys. J.* **720**, 1073–1089 (2010).
- [17] Henry, G. W., Marcy, G. W., Butler, R. P., and Vogt, S. S.: A Transiting “51 Peg-like” Planet. *Astrophys. J.* **529**, L41–L44 (2000).
- [18] Hewish, A.: Pulsars. *Scientific American* **219**, 25–35 (1968).
- [19] Kiefer, F., Lecavelier des Etangs, A., Boissier, J., Vidal-Madjar, A., Beust, H., Lagrange, A.-M., Hébrard, G., and Ferlet, R.: Two families of exocomets in the  $\beta$  Pictoris system. *Nature* **514**, 462–464 (2014).
- [20] Latham, D. W., Stefanik, R. P., Mazeh, T., Mayor, M., and Burki, G.: The unseen companion of HD114762 - A probable brown dwarf. *Nature* **339**, 38–40 (1989).
- [21] Marcy, G. W., and Benitz, K. J.: A search for substellar companions to low-mass stars. *Astrophys. J.* **344**, 441–453 (1989).
- [22] Marcy, G. W., and Butler, R. P.: A Planetary Companion to 70 Virginis. *Astrophys. J.* **464**, L147 (1996).
- [23] Mayor, M., and Queloz, D.: A Jupiter-Mass Companion to a Solar-Type Star. *Nature* **378**, 355 (1995).
- [24] Paczynski, B.: Gravitational microlensing by the galactic halo. *Astrophys. J.* **304**, 1–5 (1986).
- [25] Sahlmann, J., Ségransan, D., Queloz, D., Udry, S., Santos, N. C., Marmier, M., Mayor, M., Naef, D., Pepe, F., and Zucker, S.: Search for brown-dwarf companions of stars. *Astron. Astrophys.* **525**, A95 (2011).
- [26] Street, R. A., Udalski, A., Calchi Novati, S., Hundertmark, M. P. G., Zhu, W., Gould, A., Yee, J., Tsapras, Y., Bennett, D. P., RoboNet Project, T., Consortium, M., Jørgensen, U. G., Dominik, M., Andersen, M. I., Bachelet, E., Bozza, V., Bramich, D. M., Burgdorf, M. J., Cassan, A., Ciceri, S., D’Ago, G., Dong, S., Evans, D. F., Gu, S.-H., Harkonnen, H., Hinse, T. C., Horne, K., Figuera Jaimes, R., Kains, N., Kerins, E., Korhonen, H., Kuffmeier, M., Mancini, L., Menzies, J., Mao, S., Peixinho, N., Popovas, A., Rabus, M., Rahvar, S., Ranc, C., Tronsgaard Rasmussen, R., Scarpetta, G., Schmidt, R., Skottfelt, J., Snodgrass, C., Southworth, J., Steele, I. A., Surdej, J., Unda-Sanzana, E., Verma, P., von Essen, C., Wambsganss, J., Wang, Y.-B., Wertz, O., OGLE Project, T., Poleski, R., Pawlak, M., Szymanski, M. K., Skowron, J., Mroz, P., Kozłowski,



- S., Wyrzykowski, L., Pietrukowicz, P., Pietrzynski, G., Soszynski, I., Ulaczyk, K., The Spitzer Team Beichman, C., Bryden, G., Carey, S., Gaudi, B. S., Henderson, C., Pogge, R. W., Shvartzvald, Y., The MOA Collaboration, Abe, F., Asakura, Y., Bhattacharya, A., Bond, I. A., Donachie, M., Freeman, M., Fukui, A., Hirao, Y., Inayama, K., Itow, Y., Koshimoto, N., Li, M. C. A., Ling, C. H., Masuda, K., Matsubara, Y., Muraki, Y., Nagakane, M., Nishioka, T., Ohnishi, K., Oyokawa, H., Rattenbury, N., Saito, T., Sharan, A., Sullivan, D. J., Sumi, T., Suzuki, D., Tristram, P. J., Wakiyama, Y., Yonehara, A., KMTNet Modeling Team Han, C., Choi, J.-Y., Park, H., Jung, Y. K., and Shin, I.-G.: Spitzer Parallax of OGLE-2015-BLG-0966: A Cold Neptune in the Galactic Disk. ArXiv e-prints, (2015).
- [27] Sumi, T., Kamiya, K., Bennett, D. P., Bond, I. A., Abe, F., Botzler, C. S., Fukui, A., Furusawa, K., Hearnshaw, J. B., Itow, Y., Kilmartin, P. M., Korpela, A., Lin, W., Ling, C. H., Masuda, K., Matsubara, Y., Miyake, N., Motomura, M., Muraki, Y., Nagaya, M., Nakamura, S., Ohnishi, K., Okumura, T., Perrott, Y. C., Rattenbury, N., Saito, T., Sako, T., Sullivan, D. J., Sweatman, W. L., Tristram, P. J., Udalski, A., Szymański, M. K., Kubiak, M., Pietrzyński, G., Poleski, R., Soszyński, I., Wyrzykowski, L., Ulaczyk, K., and Microlensing Observations in Astrophysics (MOA) Collaboration: Unbound or distant planetary mass population detected by gravitational microlensing. *Nature* **473**, 349–352 (2011).
- [28] Tinetti, G., Vidal-Madjar, A., Liang, M.-C., Beaulieu, J.-P., Yung, Y., Carey, S., Barber, R. J., Tennyson, J., Ribas, I., Allard, N., Ballester, G. E., Sing, D. K., and Selsis, F.: Water vapour in the atmosphere of a transiting extrasolar planet. *Nature* **448**, 169–171 (2007).
- [29] Wolszczan, A.: Discovery of pulsar planets. *New Astron.* **56**, 2–8 (2012).